Bound And Free Water In Surfactant Micelles And Lipid Vesicles

Michel Picquart*, Donato Valdez*, Humberto Vázquez*, Wladimir Urbach¶ and Marcel Waks¶

*Universidad Autónoma Metropolitana-Iztapalapa, Departamento de Física, Apdo. Post. 55-534, México, DF 09340, México
¶ Laboratoire d'Imagerie Paramétrique, CNRS UMR 7623, 15 rue de l'Ecole de Médecine, F-75006 Paris, France

Abstract. Inverse micelles of surfactant AOT at low water contents are studied. From RMN measurements the molar fraction of bound water was obtained. Ultrasonic measurements, which depend on the compressibility, permit to determine the internal radius (water radius) of the micelles. With both results, the size of the bound water layer in this system was found around 0.3 nm. Correlated changes in the FT-IR absorption spectra give us information about the interaction between water and the polar head of AOT. Multilamellar vesicles, at different concentrations, of phospholipid DPPC, studied by DSC and FT-IR present a sub-zero transition near –40ºC. This transition is attributed to the interstitial water, i.e. the water confined between two DPPC bilayers. These results emphasize the peculiar properties of the bound water in such systems.

INTRODUCTION

Water plays a fundamental role in the formation and in the structure of organized molecular assemblies. Although there is a general agreement about the crucial importance of water in major biological processes, yet it is extremely difficult to understand these effects on a molecular level.

Many aqueous systems studied are relevant for understanding the behavior the water in organized molecular assemblies in the systems biological. One of these used to control water confinement is generally designated as reverse micelles or micro-emulsions. Reverse micelles are water microdroplets of variable size, dispersed in non miscible non-polar solvents and stabilized by a monolayer of surfactant. The size of these droplets, which are in thermal equilibrium, depends only on water concentration defined as the water-to-surfactant molar ratio W_0. When water is added to the surfactant solution, the micelles swell and their radius increases independently of the concentration of droplets [1].

Ionic and nonionic surfactants in solvents organics can solubilize large amounts of water by forming thermodynamically stable micro-aggregates [2]. Their environment, constituted by a continuous organic phase, offers an adequate medium for biotransformations, which have found many applications [3-4], they have also been used as membrane mimetic systems.

CP759, *Materials Science and Applied Physics: 2nd Mexican Meeting on Mathematical and Experimental Physics,*
edited by J. L. Hernández-Pozos and R. Olayo-González

Restrictive environments are known to favorably facilitate many chemical and physical processes. The efficiency of biological reactions, such as electron and the proton transfer, is attributed, in part, to the highly structured environments in which they take place. [5]. To investigate the effects of structured environments on chemical dynamics, it is advantageous to choose simple models with well-characterized physical chemical attributes [6].

Detailed NMR investigation for ionic and nonionic reversed micelles have been reported by various authors, and recently Amararene [7] from water proton NMR studies of H_2O-AOT in isooctane and decane corroborated the existence of three distinct states of water: bound water, trapped water, and apparently free water-existing in the water core of the reverse micelles droplet.

In the present work we described the analysis of chemical shift by SAXS, NMR and FT-IR absorption studies obtained with surfactants reverse micelles of AOT and DSC results on multilamellar vesicles of DPPC are also presented.

MATERIALS AND METHODS

The anionic surfactant AOT [sodium bis(2-ethylhexyl) sulfosuccinate] was purchased from Sigma (99% purity) and used after desiccation in vacuum over phosphorus pentoxide (Sicapent from Merck). Decane, Pro Analysis grade, was from Merck (>99% purity). Water used was obtained from a MilliQ system. Concentration of surfactant is expressed by

$$W_0 = \frac{\left[C_{H_2O}\right]}{\left[C_{AOT} - CMC_{AOT}\right]}$$

where CMC is the critical micellar concentration.

Samples for SAXS were filled at 25 °C in Lindeman 1-mm diameter capillaries and sealed. Experiments were performed using the $\lambda_{K\alpha}$ = 1.54 Å wavelength. Values of the radius, R were obtained from a curve fitting of $q^4 I(q)$ by a least-squares method.

Chemical shifts measurements were referenced with $TSPD_4$. A crystal of 3-(trimethylsilyl) propionic-2,2,3,3-d_4 acid (sodium salt), was used as an internal reference for the proton shifts. The experiments were carried out at 500 MHz for ^1H, at 25°C, on a Bruker AMX 500 spectrometer equipped with a Silicon Graphics workstation. If one assumes mono-dispersity and spherical shape of the reverse micellar droplets, it can be said that the observed chemical shifts of water proton magnetic resonances are the sum of the weighted average shifts of the bound water protons and free water protons present inside the droplet, i.e.: $\delta = \delta_B P_B + \delta_F P_F$, where δ, δ_B, and δ_F are the observed chemical shifts and the chemical shifts of bound and free water protons, respectively. P_B and P_F are the mole fractions of bound and free water, respectively, inside the water core.

Commercial sample of 1,2-hexadecanoyl-sn-glycero-3-phosphocholine (DPPC) was purchased from Sigma (99% purity). As isomer positional purity (at the glycerol backbone) is 98%, it was used without further purification.

DPPC multilayers were prepared by dissolving lipid powder in analytical grade chloroform from Prolabo. The solvent was evaporated at 60ºC under nitrogen stream and the resulting dry film stored for at least ten hours in a desiccator under vacuum. Triply distilled water has been added, and the sample steered during five minutes

beyond 45°C. This treatment was repeated three times. Samples prepared following this method gave the more intense sub-zero transition enthalpies.

DSC experiments were carried out using a DSC-10 TA instruments (USA) calorimeter equipped with a computer-analyzer system. Transition, crystallization and melting temperatures correspond to the computed peak-onset temperatures. Sample masses varied between 5 and 25 mg and were sealed in aluminum pans. Each sample crucible was placed, together with a reference one, into the DSC-cell purged by a dry nitrogen gas stream in order to prevent water vapor condensation during the low-temperature measurements. The cooling rate and the heating rate were 3°C/min. The accuracy for enthalpy changes is better than 5% after DSC energy calibration.

The AOT preparations were placed in a VC-01 variable path-length cell from Beckman equipped with CaF_2 windows. DPPC samples were placed directly between CaF_2 windows with a path-length of 7 or 6 μm. FT-IR experiments were carried out on a Nicolet 5DX spectrometer equipped with a TGS detector. Cooling was performed with a liquid nitrogen bath. The cooling and heating rates could not be accurately controlled but the former was around 1.5°C/min and the latter around 0.5°C/min. For each spectrum, 20 scans at 4 cm^{-1} resolution were collected, coadded, apodized with a Happ-Genzel function, and Fourier transformed.

RESULTS AND DISCUSION

Experimental results of SAXS, NMR and FT-IR of inverse micelles of AOT and DSC of multilamellar vesicles of DPPC will be presented hereafter.

Inverse micelles of AOT

SAXS and NMR techniques have been used to determine the content of water inside of the AOT reverse micelle solutions. A SAXS plot of an AOT-decane solution is presented in Fig. 1 for $W_0 = 9$. The internal core radius is directly calculated from

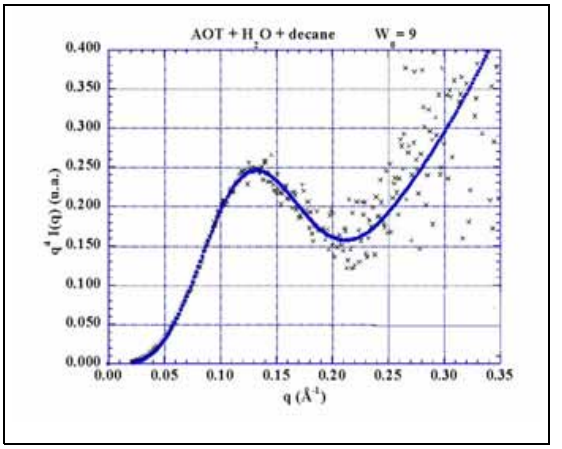

FIGURE 1. Plot of $q^4 I(q)$ of a microemulsion of AOT at $W_0 = 9$ in function of the wave vector at 25ºC.

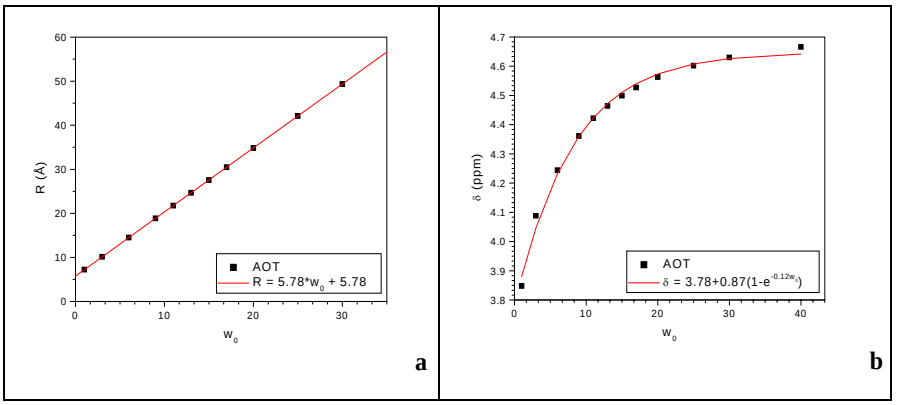

FIGURE 2. Plot of the Radius (a) and chemical shift (b) of solutions of AOT as a function of the hydration at 25ºC.

the maximum of this curve. The results are given in the Fig. 2a in function of the hydration W_0. A lineal relation between the water core radius and the molar ratio W_0 is obtained. An extrapolation to zero hydration gave us an AOT micelle radius equal to 5.38 Å.

The chemical shift of the water proton of AOT solutions in function of the water content W_0 is presented in Fig. 2b at 25ºC. An exponential dependence is found. At higher water content the chemical shift tends to 4.65 (± 0.03) ppm, in agreement with previous works [8-9]. At "zero" water content a value of 3.78 (± 0.03) ppm is found, that could be attributed to bound water, which indicates probably some residual water molecules inside the AOT powder.

This residual water is also observed by FT-IR in the OH stretching region (Fig. 3c) and in the OH deformation region (Fig. 3b). In Fig. 3b we can observe a band near 3195 cm^{-1} that can be attributed to ν_{OH} of bound water. This band is also observed at $W_0 = 0$. When the water content increased the absorptions at 3445 and 3600 cm^{-1}, usually observed in bulk water, increased [10]. At higher water content the lowest frequency band merged into these two bands. In bulk water these bands are found at 3240, 3400 and 3630 cm^{-1}, respectively.

In the δ_{OH} region (Fig. 3b), residual water is also encountered at $W_0 = 0$. Moreover two bands are observed at 1624 and 1650 cm^{-1}. In bulk water, only one band is found at 1645 cm^{-1}. AOT molecule contains two C=O groups that give two different absorptions at 1720 and 1738 cm^{-1} at low water content. When the hydration is increased to $W_0 = 15$ only one band is observed at 1734 cm^{-1}. These changes are due to the fact that the two C=O groups are not equivalent and to the change of conformation of the AOT polar group which has a *trans*-like conformation at low water content and a *gauche*-like conformation at higher water content [11]. The two deformation bands observed for water could be due to the different environment of the two C=O groups.

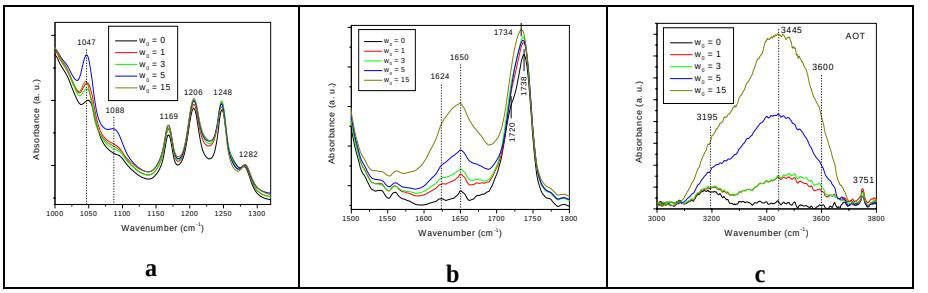

FIGURE 3. FT-IR absorption spectra of AOT solutions in function of hydration (increased hydration upward): a) 1000 – 1350 cm^{-1} region, b) 1500 – 1800 cm^{-1} region, and c) 300 – 3800 cm^{-1} region.

Finally on Fig. 3a are shown the bands due to the C-C bonds between 1250 and 1300 cm^{-1} and two bands due to the SO_3 group at 1047 and 1088 cm^{-1} where a low wavenumber shift is observed upon hydration.

Multilamellar vesicles of DPPC

In fig. 4 a complete cycle between +50°C and -60°C obtained by DSC for an aqueous dispersion of DPPC (83% in-mass of water) is shown with all the phase transitions: the main water crystallization near -15°C, the sub-zero phase transition at -40°C, the melting of ice at 0°C, as well as the pre-transition and the main transition of DPPC at 35 and 41°C, respectively.

This thermogram leads one to conclude that, if the pre-transition and main transition are not affected by this cyclic thermal treatment, the system must be in the gel phase $L_{\beta'}$ just after melting of ice. This means that the « reversible » sub-zero phase transition is necessarily hidden by the melting of ice on heating. This is confirmed by the $\Delta H'_f \approx \Delta H_f - \Delta H_{sub}$, where $\Delta H'_f$ is the enthalpy of melting of ice, ΔH_{sub} the enthalpy of the sub-zero phase transition, and ΔH_f the enthalpy of melting when the sample is cooled to -30°C. So, ΔH_f represents the melting of water molecules which are not involved in the sub-zero phenomenon.

The use of FT-IR has been performed on this system in order to determine which molecular vibrations are involved [12]. Infrared results give direct evidence that water is involved in the sub-zero phase transition. Conversely, the phospholipid molecules do not seem to take part of it since their vibrational spectra are affected neither in the polar region nor in the hydrophobic one.

Consequently, the enthalpy of the reversible sub-zero phase transition ΔH_{sub} is assumed to be equal to the crystallization enthalpy of water at the sub-zero transition temperature. It is then possible to evaluate both the number of water molecules involved in the sub-zero phase transition and that of the molecules which melt at 0°C. The number of water molecules (n_{nc}) which do not crystallize at least down to -60°C is given by:

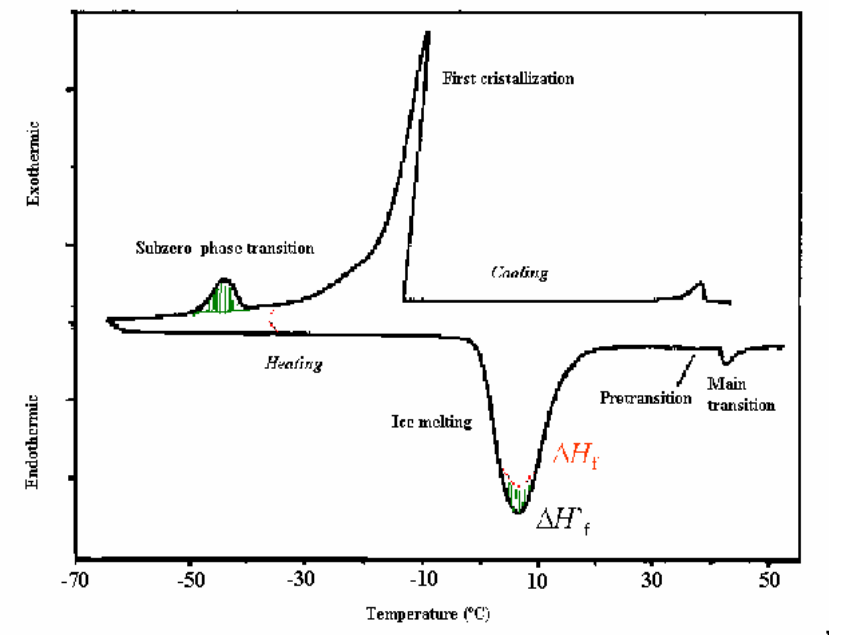

FIGURE 4. DSC thermogram between –60ºC and 50ºC for an aqueous solution of DPPV (83% water by height). The dotted line is the thermogram obtained when the sample is cooled only to –35ºC and then heated (with permission of European Biophysics Journal, Crystallization of water in multilamellar vesicles, by T. Lefèvre, S. Toscani, M. Picquart, and J. Dugué, 31, 126-134, figure 4, 2002, Springer ©EBSA 2001).

$$n_{nc} = \left(1 - \frac{\Delta H'_f}{\Delta H_w}\right) c$$

where ΔH_w is the enthalpy of melting of ice (333 J/g) and c is the ratio of the number of water molecules to that of DPPC molecules. It is found that n_{nc} keeps a nearly constant value around 8-10 H_2O/DPPC molar ratio. This result is in agreement with those of Grdadolnik *et al.* [13].

Then the number of water molecules which are not involved (n_f), and those which are involved (n_{sub}) in the sub-zero phase transition are given by:

$$n_{sub} = \left[\left(1 - \frac{\Delta H_f}{\Delta H_w}\right) c\right] - n_{nc}$$

and

$$n_f = \frac{\Delta H_f}{\Delta H_w} c,$$

respectively.

A plot of the relative number of water molecules n_{sub}/c vs. water content expressed in terms of c is shown on Fig. 5. This curve shows a maximum for 27 H_2O/DPPC (40% of water mass) and n_{sub}/c tends towards zero for high and low water concentrations. n_{sub} is found nearly constant and equal to 8 H_2O/DPPC moles. This

number has to correspond to the number of interstitial (bounded) water molecules except the ones of the molecules which do not crystallize.

These results are suggesting that the first crystallization involves the bulk phase and that the sub-zero transition is concerned with the crystallization of interstitial or bound water, except 8-10 H_2O/DPPC molecules which do not crystallize and seem to be involved in

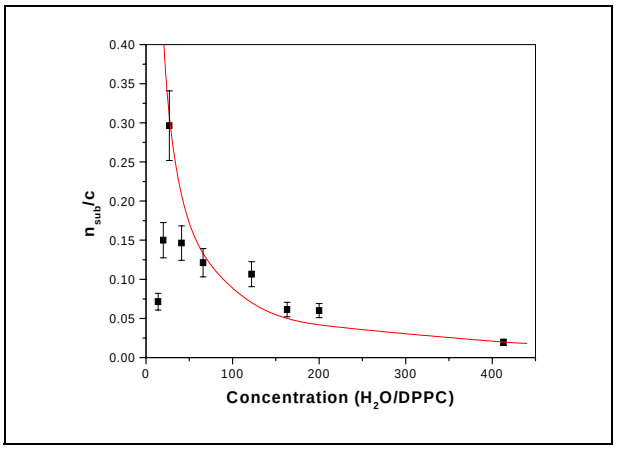

FIGURE 5. Variation of the sub-zero transition water (n_{sub}/c) versus the water concentration (c). The line represents this number, for the same samples, if 8 H_2O/DPPC are implicated. (with permission of European Biophysics Journal, Crystallization of water in multilamellar vesicles, by T. Lefèvre, S. Toscani, M. Picquart, and J. Dugué, 31, 126-134, figure 5, 2002, Springer ©EBSA 2001).

the formation of DPPC hydrates [14]. Identical experiments were performed with D_2O as solvent and with an unsaturated phospholipid (OPPC) [12] with the same experimental observations.

CONCLUSIONS

In this report we provide insights on confinement properties in membrane-mimetic systems. These results are relevant to study the physical-chemical properties of water at biological interfaces involved in major physiological mechanisms. In both systems presented here, the results are in agreement. Three kind of water are encountered. Some water molecules are always present even in dry samples of land never participate to crystallization and melting processes and the on heating process. Other water molecules (bounded water) which participate to the ice melting have peculiar properties and frozen at lower temperatures than bulk water. The third kind of water is bulk water. We can suggest that interstitial or bound water must be more structured than bulk water to need a lower crystallization temperature. The reasons of bonding are the electrostatic interactions between polar heads and water molecules. If we think in biological cells then an important question occurs: what happens in these systems as it is known that the cells and all the internal organites are composed of membranes

with polar heads. Finally, what are the physiological consequences of a such layer of bounded water?

ACKNOWLEDGMENTS

This research was supported in part by Consejo Nacional de Ciencia y Tecnología (México) program and by Centre National de la Recherche Scientifique (France) program.

REFERENCES

1. Amararene, A., Gindre, M. LeHuérou, J.Y., Urbach, W. and Waks, M., *J. Phys. Chem. B* **101**, 10751-10756 (1997).
2. Merdas, A., Gindre, M. Ober, R., Nicot, C., Urbach, W. and Waks, M., *J. Phys. Chem. B* **100**, 15180-15186 (1996).
3. Oldfield, C., *Biotechnol. Genet. Engin. Rev.* **12**, 255- (1994).
4. Komives, C.F., Lilley, E. and Russel, A.J., *Biotechnol. Bioeng.* **43**, 946-959 (1994).
5. Stryer, L., *Biochemistry*, New York: Freeman, 1995.
6. Riter, R.E., Willard, DF.M.and Levinger, N.E., *J Phys. Chem. B* **102**, 2705-2714 (1998).
7. Amararene, A., Gindre, M., LeHuérou, J.Y., Urbach, W., Valdez, D. and Waks, M., *Phys. Rev. E* **61**, 682-689 (2000).
8. White, W.T. and Finke, R.G., *J. Inorg. Biochem.* **91**, 371-387 (2002).
9. McCormick,M., Smith, R.N., Graf, R., Barret, C.J., Reven, L. and Spiess, H.W., *Macromolecules* **36**, 3616-3625 (2003).
10. Walrafen, G.E., *Water, a comprehensive treatise*, Vol. 1, edited by XXX, New York, Plenum Press, 1973, Chapter 5.
11. Christopher, D.J., Yarwood, J., Belton, P.S. and Hills, B.P., *J. Colloid Interface Sci.* **152**, 465-472 (1992).
12. Lefèvre, T., Toscani, S., Picquart, M. and Dugué, J., *Eur. Biophys. J.*, **31**, 126-134 (2002).
13. Grdadolnik, J., Kidric, J. and Hadzi, D., *J. Mol. Struct.*, **322**, 93-103 (1994).
14. Grünert, M., Börngen, L. and Nimtz, G., *Ber. Bunsunges. Phys. Chem.*, **88**, 608-612 (1984).